Convergence of Multi Point Flux Approximations on Quadrilateral Grids

Runhild A. Klausen and Ragnar Winther

Centre of Mathematics for Applications, University of Oslo, Norway

This paper presents a convergence analysis of the multi point flux approximation control volume method, MPFA, in two space dimensions. The MPFA version discussed here is the so–called O–method on general quadrilateral grids. The discretization is based on local mappings onto a reference square. The key ingredient in the analysis is an equivalence between the MPFA method and a mixed finite element method, using a specific numerical quadrature, such that the analysis of the MPFA method can be done in a finite element setting. © ??? John Wiley & Sons, Inc.

Keywords: Convergence, multi point flux approximation, mixed finite element

I. INTRODUCTION

The multi point flux approximation, MPFA, is a discretization method developed by the oil industry to be the next generation method in reservoir simulation. The goal was to replace the classical cell centered finite difference five or seven point molecule, that was, and still is, used outside its range of validity, cf. [1, 4, 15]. In reservoir simulation the geology of the reservoir, which includes faults and non parallel layers in the media, is a major challenge. This results in a need to use non-orthogonal grids, with a full discontinuous permeability tensor in the discretization. In multiphase flow a locally conservative numerical method for the elliptic pressure equation is also needed, a demand inherited from the connection to the hyperbolic saturation equation, cf. [20, 21]. In addition, it is favorable if the numerical method has a discrete explicit flux as a function of cell-centered pressure values. This enables fully implicit multiphase flow simulations. MPFA control volume methods meet all these demands, and due to this there is an increasing interest in this methodology. MPFA is already implemented in an industry standard reservoir simulator package, cf. [22]. The Galerkin finite element method is by comparison not locally conservative, while the mixed finite element method with classical elements such as Raviart-Thomas, or Brezzi-Douglas-Marini does not have an explicit flux. Even the control volume method presented in [6], which has an explicit

Numerical Methods for Partial Differential Equations ???, 1–18 (???)

two point flux approximation, does not handle a fully discontinuous permeability. Strong oscillations are shown to occur, cf. [20].

Even if there is a substantial interest for the class of MPFA methods in the reservoir engineering community, a rigorous convergence theory for these schemes have been missing. Only truncation error analysis on some idealized cases, with uniform parallelepiped grids in homogeneous media, have been done, cf. [4]. The goal of this paper is to present a convergence analysis of an MPFA method on quadrilateral grids. The MPFA version chosen is presented in a number of papers under the heading of curvilinear spaces, cf. [1, 2], and is based on local mappings onto a reference space. This is a useful feature for our analysis. A variety of numerical examples for this, and related MPFA versions can be found in papers focusing on numerical aspects, cf. [5, 15, 16, 17]. This paper is devoted to the theoretical analysis. As is common when finite volume methods are analyzed on general quadrilateral grids, the analysis will be based on a close relation to a mixed finite element method. By introducing proper finite element spaces, and a specific numerical quadrature rule, we establish an equivalence between the two methods. The finite element space, using a broken Raviart-Thomas space, is chosen such that it exactly corresponds to the MPFA's degrees of freedom, and the quadrature rule is proved to satisfy key identities, cf. Section III. C.. Thereafter, a mixed approach is used to prove linear convergence. An alternative analysis of the related mixed finite element method, using the lowest order Brezzi-Douglas-Marini elements is presented in a forthcoming paper [25, 24]. The analysis presented here is built on some mesh restrictions, and the mesh can be characterized as h^2–uniform or uniform refined. Numerical experiments verify the need for this restriction in order to avoid degeneration of the convergence order for the present MPFA version, cf. [5]. This is exactly the same restriction as needed for standard mixed finite element methods on quadrilateral meshes, cf. [8].

In this paper the analysis is restricted to two space dimensions. Let Ω be a bounded domain in $\boldsymbol{R}^2$, with polygonal boundary $\partial\Omega$. The problem discussed in this paper is the elliptic equation,

$$-\mathrm{div}\,(\boldsymbol{K}(\boldsymbol{x})\mathrm{grad}\,p) = g \text{ in } \Omega, \tag{1.1}$$

$$p(\boldsymbol{x}) = 0 \text{ on } \partial\Omega.$$

This is to be viewed as a prototype for the pressure equation in a reservoir simulation setting. The boundary condition is chosen for simplicity of exposition. Equation (1.1) can be found from assumption of mass conservation over a control volume and Darcy's law. The terminology is adopted from the application in question, and we denote p the pressure, $\boldsymbol{K}$ the permeability, and $\boldsymbol{u} = -\boldsymbol{K}\,\mathrm{grad}\,p$ the Darcy velocity. Due to generalization to multi phase flow, some specific properties of the discretization are desirable. The method should be mass conservative and have a local explicit flux approximation. The MPFA methods meet these demands.

The MPFA discretization is a control volume formulation, where more than two pressure values are used in the flux approximation. The first derivation of the methods was published in 1994, [2] and [14]. Other references on these methods are for example [1, 3, 15]. A connection from an expanded mixed finite element method, [7], to a MPFA is shown on orthogonal grids in [21]. Based on this connection, a preliminary analysis of MPFA on quadrilateral grids is given in [20].

Convergence analysis similar to the approach given here have during recent years been given by several authors for alternative finite volume methods, cf. for example [6]. In fact, a new finite volume method was created by this approach. Another example is the convergence proof given in [12] of the control volume mixed finite element method. A convergence proof for the support operator method, proposed in [19], can also be constructed in this manner, cf. [9].

The rest of the paper is organized as follows. Section provides the basic notation and concepts needed in this paper. In Section III. the MPFA method is rewritten to give the discrete set of equations found from a mixed finite element method where a quadrature rule is applied. Section IV. contains the main error estimates for the MPFA method.

II. PRELIMINARIES

Let $L_2(E)$ denote the square Lebesgue-integrable function on the domain $E \subset \boldsymbol{R}^2$ with inner product $(\cdot\,,\cdot)_E$ and norm $\|\cdot\|_E = (\cdot\,,\cdot)_E^{1/2}$. If E equals the domain Ω of (1.1) introduced above the subscript will be dropped. Also, let $H^1(E)$ denote the Sobolev space of first order differentiable functions in $L_2(E)$, with norm

$$\|q\|_{1,E} = (\|q\|_E^2 + |q|_{1,E}^2)^{1/2},$$

and with the associated seminorm

$$|q|_{1,E} = \|\operatorname{grad} q\|_E.$$

The space

$$H(\mathrm{div};E) = \{\boldsymbol{v} \in (L_2(E))^2 : \operatorname{div}\boldsymbol{v} \in L_2(E)\},$$

is equipped with the norm

$$\|\boldsymbol{v}\|_{\mathrm{div},E} = (\|\boldsymbol{v}\|_E^2 + \|\operatorname{div}(\boldsymbol{v})\|_E^2)^{1/2}.$$

Also, let P_k be the set of polynomials of degree k. The permeability $\boldsymbol{K}$ is a symmetric tensor which is uniformly positive definite in Ω. In fact, it is an important feature of reservoir simulation that $\boldsymbol{K}$ is allowed to be discontinuous, and both the MPFA method and the mixed finite element method adapt to this case. However, for technical reasons the analysis in this paper is restricted to cases where the components of $\boldsymbol{K}$ are $C^1(\bar{\Omega})$, and the Darcy velocity is assumed to satisfy $\boldsymbol{u} \in (H^1(\Omega))^2$. This regularity is for example ensured if the domain Ω is convex, and $g \in L_2$. In special cases discontinuous coefficients still give some smoothness of the solution, and for such cases relaxed smoothness condition on the permeability is allowed.

A. Quadrilateral Meshes

Let $\{\mathcal{T}_h\}$ denote a family of partitions of Ω into quadrilateral subdomains, or cells, where h is the maximum element edge. We will assume that the family is regular, cf. [13, page 246–247], i.e. all cells are convex, the angles are uniformly bounded away from zero and π, and the ratio between the length of the smallest edge and the diameter of the cell is uniformly bounded from below. Assume further that each interior vertex of $\mathcal{T}_h$ meets four cells. Finally, denote the set of edges of $\mathcal{T}_h(\Omega)$ on Ω by $\mathcal{E}_h(\Omega)$.

In order to define the proper finite element method below we need to introduce certain finite dimensional function spaces. In particular, we shall introduce a subspace of $H(\mathrm{div})$ which can be referred to as a splitting of the lowest order Raviart-Thomas space over

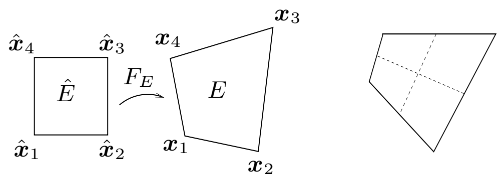

FIG. 1. To the left, the bilinear mapping F_E from $\hat{E}$ into E. To the right, a major cell and it's subcells.

a quadrilateral mesh. For any cell $E \in \mathcal{T}_h$ we will utilize a bilinear mapping $F = F_E : \hat{E} \to E$ which is smooth and invertible, see Figure 1. Here, the reference element $\hat{E} = (0,1) \times (0,1)$ is the unit square. Let $\boldsymbol{x}_i = (x_i, y_i)$, $i = 1,2,3,4$, be the four vertices of element E in counterclockwise direction as shown in Figure 1. If $\boldsymbol{x}_{ij} = (\boldsymbol{x}_i - \boldsymbol{x}_j)$ the transformation F takes the form

$$F(\hat{x}, \hat{y}) = \boldsymbol{x}_1 + \boldsymbol{x}_{21}\hat{x} + \boldsymbol{x}_{41}\hat{y} + (\boldsymbol{x}_{32} - \boldsymbol{x}_{41})\hat{x}\hat{y} \tag{2.1}$$

for $(\hat{x}, \hat{y}) \in \hat{E}$. The Jacobian matrix of F is denoted $\boldsymbol{D} = \boldsymbol{D}_E$ and $J = J_E$ the Jacobian of the mapping. As a consequence of the assumptions we have

$$c_1 h^2 \le J \le c_2 h^2, \tag{2.2}$$

and

$$|\boldsymbol{D}| \le c_3 h, \tag{2.3}$$

for constants c_i independent of h. Here $|\boldsymbol{D}|$ denote the spectral norm of the matrix $\boldsymbol{D}$.

We also assume $\{\mathcal{T}_h\}$ to be h^2–uniform, cf. [18], to recover the classical interpolation estimates. The partition $\{\mathcal{T}_h\}$ is said to be *h^2–uniform*, if there exits a constant c, independent of h, such that

$$|F_{\hat{x}\hat{y}}| = |\boldsymbol{x}_{32} - \boldsymbol{x}_{41}| \le ch^2. \tag{2.4}$$

Given a general quadrilateral grid, this is a consequence of further uniform refinement. To see this, divide all the cells of $\mathcal{T}_h$, into four subcells, by dividing each edge into two equal half edges, see Figure 1. Note that (2.1) is linear along the edges, such that dividing each cell edge into two equal parts gives the uniform refinement. The resulting refinement has cells approaching parallelogram as h decrease. Let $\boldsymbol{x}_i$, $i = 1,2,3,4$, define a given cell, and $\boldsymbol{x}'_i$, $i = 1,2,3,4$, define one of the four subcells. Then for the new refinement level

$$|F_{\hat{x}\hat{y}}| = |\boldsymbol{x}'_{32} - \boldsymbol{x}'_{41}| = \frac{1}{4}|\boldsymbol{x}_{32} - \boldsymbol{x}_{41}|$$

Hence after the grid size is halved j times, the factor $|F_{\hat{x}\hat{y}}|$ is reduced by a factor $(1/2)^{2j}$.

If $\hat{\boldsymbol{v}}$ is a vector field in $H(\mathrm{div}, \hat{E})$, define a vector field $\boldsymbol{v}$ on E by the Piola transform $\mathcal{P} = \mathcal{P}_E$, i.e.

$$\boldsymbol{v}(\boldsymbol{x}) = \mathcal{P}\hat{\boldsymbol{v}}(\hat{\boldsymbol{x}}) = \frac{1}{J}\boldsymbol{D}\hat{\boldsymbol{v}} \circ F^{-1}(\boldsymbol{x}).$$

Then $\int_E \mathrm{div}\, \boldsymbol{v}\, q\, d\boldsymbol{x} = \int_{\hat{E}} \mathrm{div}\, \hat{\boldsymbol{v}}\, \hat{q}\, d\hat{\boldsymbol{x}}$ for all $q \in L_2$ when $\hat{q} = q \circ F$. Therefore,

$$\mathrm{div}\, \hat{\boldsymbol{v}} = J\, \mathrm{div}\, \boldsymbol{v} \tag{2.5}$$

and

$$\int_e \boldsymbol{v} \cdot \boldsymbol{n}\, ds = \int_{\hat{e}} \hat{\boldsymbol{v}} \cdot \hat{\boldsymbol{n}}\, d\hat{s}, \tag{2.6}$$

where s and $\hat{s}$ denote the arc length along the edges e and $\hat{e}$, respectively, with $\boldsymbol{n}$ and $\hat{\boldsymbol{n}}$ as the unit normal vectors. Hence, the flux across each edge is preserved from the reference space to the physical space. The norms $\|\boldsymbol{v}\|_E$ and $\|\hat{\boldsymbol{v}}\|_{\hat{E}}$ are equivalent uniformly in h, while from (2.2) and (2.5),

$$c_1 h^2 \|\mathrm{div}\boldsymbol{v}\|_E^2 \le \|\mathrm{div}\hat{\boldsymbol{v}}\|_{\hat{E}}^2 \le c_2 h^2 \|\,\mathrm{div}\,\boldsymbol{v}\|_E^2. \tag{2.7}$$

For a general reference on the Piola transform we refer to [11].

Define the analog reference permeability as

$$\hat{\boldsymbol{K}} = \hat{\boldsymbol{K}}_E = \mathrm{J}\boldsymbol{D}^{-1}\boldsymbol{K}\boldsymbol{D}^{-T}. \tag{2.8}$$

Note that $\hat{\boldsymbol{K}}$ is bounded from above and below independent of h. Furthermore $\hat{\boldsymbol{K}}^{-1} = J^{-1}\boldsymbol{D}^T\boldsymbol{K}^{-1}\boldsymbol{D}$ and

$$(\boldsymbol{K}^{-1}\boldsymbol{u}, \boldsymbol{v})_E = (J\,\boldsymbol{K}^{-1}\frac{1}{J}\boldsymbol{D}\hat{\boldsymbol{u}}, \frac{1}{J}\boldsymbol{D}\hat{\boldsymbol{v}})_{\hat{E}} = (\hat{\boldsymbol{K}}^{-1}\hat{\boldsymbol{u}}, \hat{\boldsymbol{v}})_{\hat{E}}. \tag{2.9}$$

The matrix field $\hat{\boldsymbol{K}}$ embodies both the permeability and the shape of the cells, and will be an essential factor in the further discussions and results. If $\hat{\boldsymbol{K}}$ is diagonal the grid is usually referred to as a $\boldsymbol{K}$–orthogonal grid.

Since

$$J\boldsymbol{D}^{-1} = \begin{bmatrix} y_{\hat{y}} & -x_{\hat{y}} \\ -y_{\hat{x}} & x_{\hat{x}} \end{bmatrix} \tag{2.10}$$

any first order derivative of this matrix field will, by (2.1), be bounded by $|F_{\hat{x}\hat{y}}|$. Hence, using(2.4),

$$\left|(J\boldsymbol{D}^{-1})_{\hat{x}}\right|, \left|(J\boldsymbol{D}^{-1})_{\hat{y}}\right| \le ch^2. \tag{2.11}$$

Let $\bar{\boldsymbol{v}} = \boldsymbol{v} \circ F_E$. Then

$$\begin{aligned} |\hat{\boldsymbol{v}}|_{1,\hat{E}}^2 &\le c\left(\|J\boldsymbol{D}^{-1}\|_{\infty,\hat{E}}^2 |\bar{\boldsymbol{v}}|_{1,\hat{E}}^2 + |F_{\hat{x}\hat{y}}|^2 \|\bar{\boldsymbol{v}}\|_{\hat{E}}^2\right) \\ &\le c\left(h^2|\bar{\boldsymbol{v}}|_{1,\hat{E}}^2 + h^4\|\bar{\boldsymbol{v}}\|_{\hat{E}}^2\right) \\ &\le ch^2\|\boldsymbol{v}\|_{1,E}^2. \end{aligned} \tag{2.12}$$

Similarly, any first order derivative of the Jacobian J is $O(h^3)$ for h^2–uniform grids. To see this, note that the Jacobian is linear, with

$$\begin{aligned} J =& (x_{21}y_{41} - x_{41}y_{21}) + (x_{21}(y_{32} - y_{41}) - (x_{32} - x_{41})y_{21})\hat{x} \\ &+ ((x_{32} - x_{41})y_{41} - x_{41}(y_{32} - y_{41}))\hat{y}, \end{aligned}$$

and this gives $|J_{\hat{x}}|, |J_{\hat{y}}| \le ch^3$. Let $\bar{r} = \mathrm{div}\,\boldsymbol{v} \circ F_E$, such that $\mathrm{div}\,\hat{\boldsymbol{v}} = J\bar{r}$. Then

$$\begin{aligned} |\mathrm{div}\,\hat{\boldsymbol{v}}|_{1,\hat{E}}^2 &\le c\left(\|J\|_{\infty,\hat{E}}^2|\bar{r}|_{1,\hat{E}}^2 + \|\,\mathrm{grad}\,J\|_{\infty,\hat{E}}^2\|\bar{r}\|_{\hat{E}}^2\right) \\ &\le c\left(h^4|\bar{r}|_{1,\hat{E}}^2 + h^6\|\bar{r}\|_{\hat{E}}^2\right) \\ &\le ch^4\|\mathrm{div}\,\boldsymbol{v}\|_{1,E}^2. \end{aligned} \tag{2.13}$$

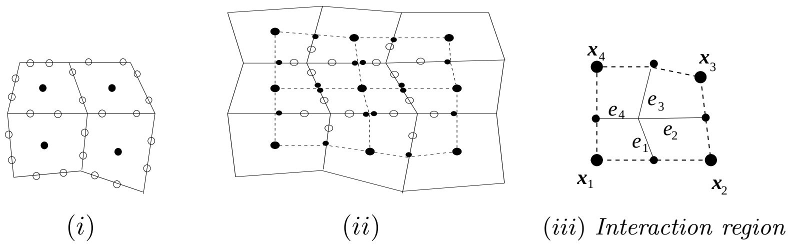

FIG. 2. To the left, (i), the degree of freedom associated with the MPFA method. The cell centered filled dots denote the cell pressure. The open dots denote the flux, and is calculated for each half cell edge. In the middle, (ii), four interaction regions, doted lines, and the underlying grid. The smaller filled dots denote the continuity point for the pressure on the edges, which are eliminated in order to find the transmissibilities. To the right (iii), one interaction region with main vertices $\boldsymbol{x}_i$ and half cell edges e_i, $i = 1, 2, 3, 4$.

For later reference, also note that in the physical space we have the estimates

$$\left|(J\boldsymbol{D}^{-1})_x\right|, \left|(J\boldsymbol{D}^{-1})_y\right| \leq ch, \quad \text{and} \quad |J_x|, |J_y| \leq ch^2. \tag{2.14}$$

Remark. *The need for h^2–uniform grids is consistent with numerical results, presented for example in [5]. There we observe that the present method may diverge on less regular grids.*

III. THE MULTI POINT FLUX APPROXIMATION

The MPFA discretization is a control volume formulation, where more than two pressure values are used in the flux approximation. The unknowns are the cell pressures, and the half edge fluxes, cf. Figure 2 (i).

Define a dual grid, $\mathcal{I}_h$, where the dual cells, denoted interaction regions $I \in \mathcal{I}_h$, consisting of the four subcells, as defined in Section A., with a common vertex, cf. Figure 2 (ii). Furthermore let $\mathcal{E}_h^{1/2}(\Omega)$ be the set of all half edges created by dividing the edges of $\mathcal{E}_h(\Omega)$ into two equal parts.

The MPFA method which we shall analyze can be written in a control volume form as

$$\begin{aligned} u_k &= \sum_{E_i \in \mathcal{T}_h} t_{k,i}\, p_i, && \text{for all } e_k \in \mathcal{E}_h^{1/2}, \\ \sum_{e_k \in \mathcal{E}_h^{1/2}(E)} u_k &= \int_E g\, d\boldsymbol{x}, && \text{for all } E \in \mathcal{T}_h. \end{aligned} \tag{3.1}$$

Here u_k is the flux across e_k, and p_i the cell pressure in cell E_i. The transmissibility coefficients $t_{k,i}$ are given by (3.14). These coefficients are zero when the half edge e_k does not belong to an interaction region containing a subcell from the primal cell E_i. The second equation of (3.1) is the exact divergence on the control volume or cell E. Hence, the entire approximation is the pressure to flux relation, given by the first equation of (3.1).

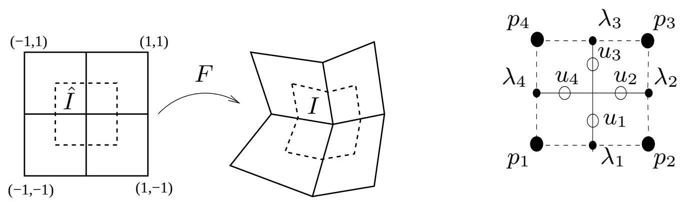

FIG. 3. To the left: Four cells with common vertex and the corresponding interaction region in the reference and physical space. To the right: One interaction region with four sub cells, numbered 1 to 4, in the reference space, where ● denotes the cell pressures $\{p_i\}$, the small • the edge pressure $\{\lambda_i\}$, and ∘ the edge velocities $\{u_i\}$.

Before the transmissibilities are calculated the transformation from Section A. into the reference space is applied. If $\boldsymbol{n}_e$ and $\hat{\boldsymbol{n}}_e$ are the edge unit normals we have from (2.6) that

$$u_e \equiv -\int_e \boldsymbol{K} \operatorname{grad} p \cdot \boldsymbol{n}_e \, ds = -\int_{\hat{e}} \hat{\boldsymbol{K}} \operatorname{grad} \hat{p} \cdot \hat{\boldsymbol{n}}_e \, d\hat{s} \equiv \hat{u}_e, \tag{3.2}$$

with $\hat{\boldsymbol{K}}$ defined in (2.8) and $\hat{p} = p \circ F_E(\hat{\boldsymbol{x}})$.

A. The Multi Point Flux Approximation on Mixed Form

Here we derive the MPFA method in a formulation that will match a version of the mixed finite element method. In this form the explicit MPFA flux is found by inverting a local 4×4 matrix. Note that $\hat{\boldsymbol{K}}$ is independent of any translation of the reference mapping F_E, equation (2.1), from Section II.. For calculations of (3.2) the reference mapping can therefore be adjusted for four and four cells with one common vertex, so that we have a reference interaction region, $\hat{I}$, see Figure 3. Denote the subcells of $\hat{I}$ for $\hat{E}_i$ and the inner subcell edges for e_i, $i = 1, 2, 3, 4$. Evaluate $\hat{\boldsymbol{K}}_E$, for all $E \in \mathcal{T}_h$, in the midpoint of the reference cell, and denote this $\mathcal{K}_E$ with components k^E_{ij}, $i, j = 1, 2$, and similar let κ^E_{ij} be the components of $\mathcal{K}_E^{-1}$.

Define the pressure space $P(\hat{I})$ on the interaction region $\hat{I}$ to be all linears on the subcells $\hat{E}_i$, which are continuous on the boundary of $\hat{I}$. For each $\hat{p} \in P(\hat{I})$ let $\{p_k\}_{k=1,2,3,4}$ be the values of $\hat{p}$ at the corners of $\hat{I}$, and $\{\lambda_k\}_{k=1,2,3,4}$ the values of $\hat{p}$ at midpoints of the edges of the boundary of $\hat{I}$, see Figure 3. The local pressure $\hat{p}$ is then uniquely defined by the eight degrees of freedom $\{p_k, \lambda_k\}$. Let

$$u_e|_{E_i} = -\mathcal{K}_i \operatorname{grad} \hat{p}|_{E_i} \cdot \hat{\boldsymbol{n}}_e /2 \tag{3.3}$$

for the two subcells E_i meeting each of the four inner edges e. The MPFA pressure space, $P_{\mathrm{MPFA}}(\hat{I})$, is further restricted to

$$P_{\mathrm{MPFA}}(\hat{I}) = \{\hat{p} \in P(\hat{I}) : [u_e]_e = 0, \ \forall e \in \mathcal{E}^{1/2}(\hat{I})\}, \tag{3.4}$$

where $\mathcal{E}^{1/2}(\hat{I})$ represents the four inner edges of $\hat{I}$, $[\,\cdot\,]_e$ is the jump across edge e, and u_e is defined by (3.3).

Lemma 3.1. *The pressure $\hat{p} \in P_{\mathrm{MPFA}}(\hat{I})$ is uniquely determined by the cell pressures $\{p_k\}_{k=1,2,3,4}$.*

The proof can be found at the end of this section.

The first relation of (3.1), the pressure to flux relation, is exactly the map taking $\{p_k\}$ to $\{u_k\}$ for $\hat{p} \in P_{\text{MPFA}}$. This map can now be characterized locally on each interaction region. In order to find this characterization, define the gradient variables $\{g_1^i, g_2^i\}_{i=1,2,3,4}$ by

$$\begin{pmatrix} g_1^i \\ g_2^i \end{pmatrix} = -\operatorname{grad}(\hat{p})/2|_{\hat{E}_i}, \qquad i = 1,2,3,4, \tag{3.5}$$

where $g_j^i \in P_0(\hat{E}_i)$, the zero order polynomial on $\hat{E}_i$. Consider the two subcells E_1 and E_2 with node pressure p_1 and p_2, and their common half edge e_1, see Figure 3. Calculating the flux u_1 across half edge e_1 on subcell E_1 gives

$$u_1 = -\mathcal{K}_1 \operatorname{grad}(\hat{p})|_{E_1} \cdot \begin{pmatrix} 1 \\ 0 \end{pmatrix} /2 = k_{11}^1 g_1^1 + k_{12}^1 g_2^1 \tag{3.6}$$

and similar the flux for across the half edge e_4,

$$u_4 = k_{22}^1 g_2^1 + k_{12}^1 g_1^1. \tag{3.7}$$

This can be written

$$\begin{pmatrix} u_1 \\ u_4 \end{pmatrix} = \mathcal{K}_1 \begin{pmatrix} g_1^1 \\ g_2^1 \end{pmatrix}, \text{ or } \begin{pmatrix} g_1^1 \\ g_2^1 \end{pmatrix} = \mathcal{K}_1^{-1} \begin{pmatrix} u_1 \\ u_4 \end{pmatrix} \tag{3.8}$$

if we solve for the gradient variables.

In the reference space, the constant gradient can be determined in each subcell between the node pressure and one point on each half edge. Let p_1 be the node pressure of cell 1 and the pressure at the midpoint of the actual edge be λ_1, see Figure 3. Using (3.5) on subcell 1 and 2 gives

$$\begin{pmatrix} g_1^1 \\ g_2^1 \end{pmatrix} = -\begin{pmatrix} \lambda_1 - p_1 \\ \lambda_4 - p_1 \end{pmatrix} \qquad \text{and} \qquad \begin{pmatrix} g_1^2 \\ g_2^2 \end{pmatrix} = -\begin{pmatrix} p_2 - \lambda_1 \\ \lambda_2 - p_2 \end{pmatrix} \tag{3.9}$$

Eliminating λ_1, gives

$$g_1^1 + g_1^2 = -(p_2 - p_1), \tag{3.10}$$

Next we use (3.8), to eliminate g_1^1 and g_1^2 to obtain the equation

$$(\kappa_{11}^1 + \kappa_{11}^2)u_1 + \kappa_{12}^1 u_4 + \kappa_{12}^2 u_2 = -(p_2 - p_1) \tag{3.11}$$

associated the edge e_1. By deriving the similar equations for the three other interior edges of $\hat{I}$ we obtain a 4×4 system of the form

$$\boldsymbol{A}\boldsymbol{u} = \boldsymbol{b}, \tag{3.12}$$

where $\boldsymbol{b} = -(p_2 - p_1, p_3 - p_2, p_3 - p_4, p_4 - p_1)^T$, $\boldsymbol{u} = (u_1, u_2, u_3, u_4)^T$, and

$$\boldsymbol{A} = \begin{pmatrix} (\kappa_{11}^1 + \kappa_{11}^2) & \kappa_{12}^2 & 0 & \kappa_{12}^1 \\ \kappa_{12}^2 & (\kappa_{22}^2 + \kappa_{22}^3) & \kappa_{12}^3 & 0 \\ 0 & \kappa_{12}^3 & (\kappa_{11}^3 + \kappa_{11}^4) & \kappa_{12}^4 \\ \kappa_{12}^1 & 0 & \kappa_{12}^4 & (\kappa_{22}^1 + \kappa_{22}^4) \end{pmatrix}. \tag{3.13}$$

Since each $\mathcal{K}_E$, $E = 1,2,3,4$ are positive definite, so is $\boldsymbol{A}$. The transmissibility coefficients $t_{k,i}$ in (3.1) are now given as the component of $\boldsymbol{T}$, where

$$\boldsymbol{u} = \boldsymbol{A}^{-1}\boldsymbol{b} = \boldsymbol{T}\boldsymbol{p} \tag{3.14}$$

and $\boldsymbol{p} = (p_1, p_2, p_3, p_4)^T$

Proof. *Lemma 3.1*. It is enough to show that if $\hat{p} \in P_{\text{MPFA}}(\hat{I})$, with $\{p_k\}_{k=1,2,3,4}$ all equal zero, then $\{\lambda_k\}_{k=1,2,3,4}$, must also be zero. Under the assumption $p_k = 0$ it follows from (3.6) and (3.9) that the constraint of continuous flux leads to the system

$$\boldsymbol{A}'\boldsymbol{\lambda} = 0$$

with $\boldsymbol{\lambda} = (\lambda_1, \lambda_2, \lambda_3, \lambda_4)^T$ and

$$\boldsymbol{A}' = \begin{pmatrix} (k_{11}^1 + k_{11}^2) & -k_{12}^2 & 0 & k_{12}^1 \\ -k_{12}^2 & (k_{22}^2 + k_{22}^3) & k_{12}^3 & 0 \\ 0 & k_{12}^3 & (k_{11}^3 + k_{11}^4) & -k_{12}^4 \\ k_{12}^1 & 0 & -k_{12}^4 & (k_{22}^1 + k_{22}^4) \end{pmatrix}. \tag{3.15}$$

This matrix is positive definite, so $\boldsymbol{\lambda} = 0$. ∎

B. The Mixed Finite Element Method

Introduce the unknown velocity $\boldsymbol{u}$ which leads to the classical mixed formulation of equation (1.1)

$$\begin{aligned} \boldsymbol{u} &= -\boldsymbol{K}\,\text{grad}\, p, \\ \text{div}\, \boldsymbol{u} &= g. \end{aligned} \tag{3.16}$$

The mixed finite element method is a discrete version of this system. A weak formulation of the system (3.16) can be formulated as the problem of finding $(\boldsymbol{u}, p) \in H(\text{div}) \times L_2$ such that

$$\begin{aligned} (\boldsymbol{K}^{-1}\boldsymbol{u}, \boldsymbol{v}) - (p, \text{div}\, \boldsymbol{v}) &= 0, \qquad \text{for all } \boldsymbol{v} \in H(\text{div}), \\ (\text{div}\, \boldsymbol{u}, q) &= (g, q), \qquad \text{for all } q \in L_2, \end{aligned} \tag{3.17}$$

where g is assumed to be an L_2 function.

In order to show that the MPFA method (3.1) is equivalent to a mixed finite element method we will introduce a new pair of discrete spaces, $\mathcal{RT}_h^{1/2} \times Q_h$.

Let $a, b, c,$ and d be piecewise constants on $(0, 1)$, with discontinuity at the midpoint. On the reference square $\hat{E}$ the velocity space $\mathcal{RT}^{1/2} = \mathcal{RT}^{1/2}(\hat{E})$ is defined as the eight–dimensional space given as all vector fields of the form

$$\begin{pmatrix} a(\hat{y}) + b(\hat{y})\hat{x} \\ c(\hat{x}) + d(\hat{x})\hat{y} \end{pmatrix}.$$

Recall that the corresponding Raviart-Thomas space, $\mathcal{RT}$, is of the same form, but with, $a, b, c,$ and d taken as constants, so $\mathcal{RT} \subset \mathcal{RT}^{1/2}$. It is straightforward to check that if $\hat{\boldsymbol{v}} \in \mathcal{RT}^{1/2}$ and $\hat{\boldsymbol{n}}$ is a normal vector to an edge of $\hat{E}$, then $\hat{\boldsymbol{v}} \cdot \hat{\boldsymbol{n}}$ is a constant along each half edge. Furthermore, this property is preserved by the Piola transform. The corresponding finite element space, $\mathcal{RT}_h^{1/2} \subset H(\text{div})$, is now defined by

$$\mathcal{RT}_h^{1/2} := \{\boldsymbol{v} \in H(\text{div}) :\ \boldsymbol{v}|_E \in \mathcal{P}_E(\mathcal{RT}^{1/2}), \quad \forall E \in \mathcal{T}_h\}.$$

Hence, the canonical degrees of freedom for the space $\mathcal{RT}_h^{1/2}$ are $\boldsymbol{v} \cdot \boldsymbol{n}$ of each half edge in $\mathcal{E}_h^{1/2}$. These degrees of freedom lead to the corresponding dual basis for $\mathcal{RT}_h^{1/2}$. Also define the ordinary zero order Raviart–Thomas space, as described in for instance [11], by

$$\mathcal{RT}_h := \{\boldsymbol{v} \in H(\text{div}) :\ \boldsymbol{v}|_E \in \mathcal{P}_E(\mathcal{RT}), \quad \forall E \in \mathcal{T}_h\}.$$

We now obviously have $\mathcal{RT}_h \subset \mathcal{RT}_h^{1/2}$. In fact, if we let $\mathcal{RT}_{h/2}$ denote the ordinary Raviart–Thomas space on the finer subcell mesh, we have $\mathcal{RT}_h \subset \mathcal{RT}_h^{1/2} \subset \mathcal{RT}_{h/2}$. In particular, the $\mathcal{RT}_h^{1/2}$ functions can be characterized as $\mathcal{RT}_{h/2}$ functions, where for each cell the function value on the inner subcell edges are the arithmetic mean of the corresponding half cell edge values.

The pressure will be approximated by piecewise constants, on $\mathcal{T}_h$ i.e., we let

$$Q_h := \{q \in L_2 :\ q|_E \in P_0(E), \quad \forall E \in \mathcal{T}_h\}.$$

On the reference element we define $\hat{\Pi} : (H^1(\hat{E}))^2 \to \mathcal{RT}$ as the standard interpolation operators onto the four dimensional Raviart–Thomas space, cf. [11],

$$\int_{\hat{e}} (\hat{\boldsymbol{u}} - \hat{\Pi}\hat{\boldsymbol{u}}) \cdot \hat{\boldsymbol{n}}\, d\hat{s} = 0, \text{ for all edges } \hat{e} \in \mathcal{E}(\hat{E}), \tag{3.18}$$

where $\mathcal{E}(\hat{E})$ represent the four edges of $\hat{E}$. The operator $\Pi_h : (H^1)^2 \to \mathcal{RT}_h \subset \mathcal{RT}_h^{1/2}$ is then simply given by

$$\Pi_h \boldsymbol{v}|_E = \mathcal{P}_E \hat{\Pi} \mathcal{P}_E^{-1} \boldsymbol{v}. \tag{3.19}$$

It is straightforward to check, using the identity (2.5), that the operator Π_h satisfies the identity

$$(\operatorname{div}(\Pi_h \boldsymbol{v} - \boldsymbol{v}), q) = 0, \qquad \text{for all } \boldsymbol{v} \in H(\operatorname{div}),\ q \in Q_h. \tag{3.20}$$

The mixed finite element method derived from the pair $\mathcal{RT}_h^{1/2} \times Q_h$ is given by: Find $(\boldsymbol{u}_h, p_h) \in \mathcal{RT}_h^{1/2} \times Q_h \subset H(\operatorname{div}) \times L_2$ such that

$$\begin{aligned} (\boldsymbol{K}^{-1}\boldsymbol{u}_h, \boldsymbol{v}) - (p_h, \operatorname{div} \boldsymbol{v}) &= 0, && \text{for all } \boldsymbol{v} \in \mathcal{RT}_h^{1/2}, \\ (\operatorname{div} \boldsymbol{u}_h, q) &= (g, q), && \text{for all } q \in Q_h. \end{aligned} \tag{3.21}$$

C. The Quadrature Rule

In order to obtain the MPFA method as a mixed finite element method we need to replace the term $(\boldsymbol{K}^{-1}\boldsymbol{u}_h, \boldsymbol{v})_E = (\hat{\boldsymbol{K}}^{-1}\hat{\boldsymbol{u}}_h, \hat{\boldsymbol{v}})_{\hat{E}}$ in (3.21) by a quadrature formula. We define this numerical quadrature formula on the reference element $\hat{E}$, and denote it $\hat{a}_E(\,\cdot\,,\,\cdot\,)$. Remember that $\mathcal{K}_E$ is $\hat{\boldsymbol{K}}_E = J\boldsymbol{D}^{-1}\boldsymbol{K}\boldsymbol{D}^{-T}$ evaluated at the midpoint of the reference cell and that the components of $\mathcal{K}_E^{-1}$ are denoted κ_{jk}^E, $j, k = 1, 2$. For the quadrature rule we will use $\mathcal{K}_E$ to approximate $\hat{\boldsymbol{K}}_E$. The rest of the quadrature formula is derived from the trapezoidal rule. If $\hat{E}_i$, $i = 1, 2, 3, 4$ are the four subcells of $\hat{E}$, let e_{ij} denote the outer half edge of subcell $\hat{E}_i$ with the jth unit vector as a normal, cf. Figure 4. Note that if $\hat{\boldsymbol{v}} = (\hat{v}_1, \hat{v}_2) \in \mathcal{RT}^{1/2}$ the exactness of the trapezoidal rule for scalar linear functions implies that

$$\frac{1}{4}\sum_{i=1}^{4} \hat{v}_k|_{e_{ik}} = \int_{\hat{E}} \hat{v}_k d\hat{\boldsymbol{x}}, \qquad k = 1, 2. \tag{3.22}$$

Let $\hat{v}_k|_{e_{ik}} = \hat{v}_{ik}$. For $\hat{\boldsymbol{v}}, \hat{\boldsymbol{u}} \in \mathcal{RT}^{1/2}$ we now define

$$\hat{a}_E(\hat{\boldsymbol{u}}, \hat{\boldsymbol{v}}) = \frac{1}{4}\sum_{i=1}^{4}\sum_{j,k=1}^{2} \kappa_{jk}^E\, \hat{u}_{ij}\hat{v}_{ik} \tag{3.23}$$

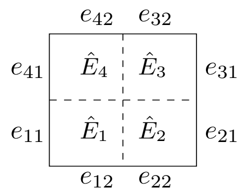

FIG. 4. One cell, with four subcells $\hat{E}_i$, and the half cell edges e_{ij}.

for functions $\hat{\boldsymbol{v}}, \hat{\boldsymbol{w}}$ in $\mathcal{RT}^{1/2}$. If $\hat{\boldsymbol{u}} \in (P_0(\hat{E}))^2$, the term $\hat{\boldsymbol{w}} = \mathcal{K}_E^{-1}\hat{\boldsymbol{u}}$ still is $(P_0(\hat{E}))^2$, then for any $\hat{\boldsymbol{v}} \in \mathcal{RT}^{1/2}$

$$\hat{a}_E(\hat{\boldsymbol{u}}, \hat{\boldsymbol{v}}) = \frac{1}{4}\sum_{k=1}^{2} \hat{w}_k \sum_{i=1}^{4} \hat{v}_{ik} = \sum_{k=1}^{2} \hat{w}_k \int_{\hat{E}} \hat{v}_k d\hat{\boldsymbol{x}} = (\mathcal{K}_E^{-1}\hat{\boldsymbol{u}}, \hat{\boldsymbol{v}})_{\hat{E}}. \tag{3.24}$$

Hence, in this case the quadrature rule is exact. The next lemma shows two important properties of the quadrature rule, which will be essential for the analysis below.

Lemma 3.2. *If $\hat{\boldsymbol{u}} \in (P_0(\hat{E}))^2$, the quadrature rule defined in* (3.23) *satisfies*

$$\hat{a}_E(\hat{\boldsymbol{u}}, \hat{\boldsymbol{v}}) = (\mathcal{K}_E^{-1}\hat{\boldsymbol{u}}, \hat{\boldsymbol{v}})_{\hat{E}} \qquad \text{for all } \hat{\boldsymbol{v}} \in \mathcal{RT}^{1/2}, \tag{3.25}$$

and

$$\hat{a}_E(\hat{\boldsymbol{u}}, (\hat{\boldsymbol{v}} - \hat{\Pi}\hat{\boldsymbol{v}})) = 0 \qquad \text{for all } \hat{\boldsymbol{v}} \in \mathcal{RT}^{1/2}. \tag{3.26}$$

Proof. Equation (3.25) follows from (3.24), since $\mathcal{K}_E^{-1}\hat{\boldsymbol{u}} \in (P_0(\hat{E}))^2$. For $\hat{\boldsymbol{v}} \in \mathcal{RT}^{1/2}$ we have

$$\sum_{i=1}^{4}((I - \hat{\Pi})v_k)|_{e_{ik}} = 0, \qquad k = 1, 2,$$

from the definition of the operator $\hat{\Pi}$. Therefore, for $\hat{\boldsymbol{u}} \in (P_0(\hat{E}))^2$ we have $\hat{u}_{ij} = \hat{u}_j$ and

$$\hat{a}_E(\hat{\boldsymbol{u}}, (I - \hat{\Pi})\hat{\boldsymbol{v}}) = \frac{1}{4}\sum_{j,k=1}^{2} \kappa_{jk}\hat{u}_j \sum_{i=1}^{4}((I - \hat{\Pi})v_k)|_{e_{ik}} = 0.$$

∎

Define the quadrature rule in the physical space as

$$a_h(\boldsymbol{v}, \boldsymbol{w}) = \sum_{\boldsymbol{E}\in\mathcal{T}_h} \hat{a}_E(\hat{\boldsymbol{v}}, \hat{\boldsymbol{w}}). \tag{3.27}$$

for all $\boldsymbol{u}, \boldsymbol{v} \in \mathcal{RT}_h^{1/2}$.

Corresponding to the approximation $\mathcal{K}_E$ of $\hat{\boldsymbol{K}}$ in the reference space, we introduce $\boldsymbol{K}_h$ in the physical space as an approximation of $\boldsymbol{K}$ given by

$$\boldsymbol{K}_h|_E = J^{-1}\boldsymbol{D}\mathcal{K}_E\boldsymbol{D}^T.$$

Note that $\boldsymbol{K}_h$ is not piecewise constant, but by construction

$$(\boldsymbol{K}_h^{-1}\boldsymbol{u},\boldsymbol{v})_E = (\mathcal{K}_E^{-1}\hat{\boldsymbol{u}},\hat{\boldsymbol{v}})_{\hat{E}}.$$

If $\bar{\boldsymbol{u}} = J\boldsymbol{D}^{-1}\boldsymbol{u}$ and $\bar{\boldsymbol{v}} = J\boldsymbol{D}^{-1}\boldsymbol{v}$, on an element E,

$$\boldsymbol{K}_h^{-1}\boldsymbol{u}\cdot\boldsymbol{v} = \mathcal{K}_E^{-1}\bar{\boldsymbol{u}}\cdot\bar{\boldsymbol{v}}/J.$$

Let $\boldsymbol{u},\boldsymbol{v} \in (P_0(E))^2$. Then from (2.2) and (2.14) any first order derivative of $\boldsymbol{K}_h^{-1}\boldsymbol{u}\cdot\boldsymbol{v}$ is bounded independent h. Since the matrix norm $|(\boldsymbol{K}^{-1} - \boldsymbol{K}_h^{-1})(\boldsymbol{x})|$ is zero at the midpoint of each cell E, and has bounded derivatives, we conclude that

$$|(\boldsymbol{K}^{-1} - \boldsymbol{K}_h^{-1})| \le ch, \tag{3.28}$$

where $|\cdot|$ is the spectral norm. The error estimate for the quadrature rule (3.27) will be given in Lemma 4.3.

D. The Mixed Finite Element Method that yields the MPFA

The last step of rewiring the MPFA as a perturbed mixed finite element method is to apply the quadrature rule on (3.27) in (3.21). We then obtain the method: Find $(\boldsymbol{u}_h, p_h) \in \mathcal{RT}_h^{1/2} \times Q_h$ such that

$$\begin{aligned} a_h(\boldsymbol{u}_h,\boldsymbol{v}) - (p_h, \operatorname{div}\boldsymbol{v}) &= 0, \qquad && \text{for all } \boldsymbol{v} \in \mathcal{RT}_h^{1/2}, \\ (\operatorname{div}\boldsymbol{u}_h, q) &= (g,q), && \text{for all } q \in Q_h. \end{aligned} \tag{3.29}$$

Theorem 3.3. *The perturbed mixed finite element method* (3.29) *is equivalent to the MPFA method from Section A..*

Proof. Recall that the space $\mathcal{RT}_h^{1/2}$ has a canonical basis derived from the degrees of freedom on each half edge in $\mathcal{E}_h^{1/2}$. It is easy to see that the mass matrix corresponding to this basis and the bilinear form a_h is block diagonal, where the 4×4 diagonal blocks correspond to the four half edges meeting a vertices of $\mathcal{T}_h$, or equivalently, to each interaction region of $\mathcal{I}_h$. Hence, by a transformation back to the reference space, the diagonal blocks resemble the structure of the matrix $\boldsymbol{A}$ given by (3.13). The second term of the first equation in (3.29) gives a pressure difference. It is a straightforward calculation to show that for each interaction region the first equation of (3.29) corresponds exactly to the system (3.12). ∎

IV. CONVERGENCE OF THE MPFA

In this final section of the paper we show the convergence of the MPFA method based on the characterization of the method given in Theorem 3.3. Hence, we will show convergence of the mixed method (3.29). However, first we will establish some necessary preliminary results.

By equivalence of norms we have

$$\|\Pi_h\boldsymbol{v}\| \le c\|\boldsymbol{v}\|, \qquad \text{for all } \boldsymbol{v} \in \mathcal{RT}_h^{1/2}, \tag{4.1}$$

where the constant c is independent of h

Lemma 4.1. *Let $\boldsymbol{v} \in (H^1)^2$, with $\operatorname{div} \boldsymbol{v} \in H^1$. Then there is a constant c, independent of h, such that*

$$\|\Pi_h \boldsymbol{v} - \boldsymbol{v}\| \leq ch\|\boldsymbol{v}\|_1, \tag{4.2}$$

$$\|\operatorname{div}(\Pi_h \boldsymbol{v} - \boldsymbol{v})\| \leq ch\|\operatorname{div} \boldsymbol{v}\|_1, \tag{4.3}$$

$$\|\mathcal{M}_h p - p)\| \leq ch\|p\|_1, \tag{4.4}$$

where $\mathcal{M}_h$ is the L_2–projection onto Q_h.

Proof. The last inequality, (4.4), is a standard estimate, and can for instance be found in [10]. The two other estimates are consequences of the assumption that $\{\mathcal{T}_h\}$ is h^2–uniform. They are derived locally on each element E of $\mathcal{T}_h$. From the equivalence of L_2–norms in Section A.,

$$\begin{aligned} \|\Pi_h \boldsymbol{v} - \boldsymbol{v}\|_E^2 &\leq c\|\hat{\Pi}\hat{\boldsymbol{v}} - \hat{\boldsymbol{v}}\|_{\hat{E}}^2 \\ &\leq c|\hat{\boldsymbol{v}}|_{1,\hat{E}}^2 \\ &\leq ch^2\|\boldsymbol{v}\|_{1,E}^2 \end{aligned}$$

from (2.12). Let $\mathcal{M}$ denote the L_2 projection onto constant functions on the reference square. To derive (4.3), start with (2.7) such that

$$\begin{aligned} \|\operatorname{div}(\Pi_h \boldsymbol{v} - \boldsymbol{v})\|_E^2 &\leq ch^{-2}\|\operatorname{div}(\hat{\boldsymbol{v}} - \hat{\Pi}\hat{\boldsymbol{v}})\|_{\hat{E}}^2 \\ &= ch^{-2}\|(I - \mathcal{M})\operatorname{div} \hat{\boldsymbol{v}}\|_{\hat{E}}^2 \\ &\leq ch^{-2}|\operatorname{div} \hat{\boldsymbol{v}}|_{1,\hat{E}}^2 \\ &\leq ch^2\|\operatorname{div} \boldsymbol{v}\|_{1,E}^2 \end{aligned}$$

from (2.13). Summing over all the elements and the Lemma follows. ■

In order to analyze the mixed method (3.29) we also need some properties of the bilinear form a_h defined on the space $\mathcal{RT}_h^{1/2}$. Using the regularity of the mesh and the equivalence of norms on the reference element $\hat{E}$ it is straightforward to show that $a_h(\boldsymbol{v}, \boldsymbol{v})^{1/2}$ is equivalent to the L_2 norm on $\mathcal{RT}_h^{1/2}$, i.e. there are constants $\alpha_0, \alpha_1 > 0$, independent of h, such that

$$\alpha_0\|\boldsymbol{v}\|^2 \leq a_h(\boldsymbol{v}, \boldsymbol{v}) \leq \alpha_1\|\boldsymbol{v}\|^2. \tag{4.5}$$

Two other central properties of the bilinear form a_h will be derived from the algebraic properties given in Lemma 3.2.

Lemma 4.2. *Let $\boldsymbol{u} \in (H^1)^2$ and $\boldsymbol{v} \in \mathcal{RT}_h^{1/2}$. Then there is a constant c, independent of h, such that*

$$|a_h(\Pi_h \boldsymbol{u}, (I - \Pi_h)\boldsymbol{v})| \leq ch\|\boldsymbol{u}\|_1\|(I - \Pi_h)\boldsymbol{v}\|.$$

Proof. Since $(I - \Pi_h)^2 = I - \Pi_h$ it is enough to show that

$$|a_h(\Pi_h \boldsymbol{u}, (I - \Pi_h)\boldsymbol{v})| \leq ch\|\boldsymbol{u}\|_1\|\boldsymbol{v}\| \tag{4.6}$$

for $\boldsymbol{u} \in (H^1)^2$ and $\boldsymbol{v} \in \mathcal{RT}_h^{1/2}$. Note also that on the reference element the bilinear form $\hat{a}_E(\hat{\Pi}\cdot, (I - \hat{\Pi})\cdot)$ is bounded on $H^1 \times \mathcal{RT}_h^{1/2}$, i.e. there is a constant c such that

$$|\hat{a}_E(\hat{\Pi}\hat{\boldsymbol{u}}, (I - \hat{\Pi})\hat{\boldsymbol{v}})| \leq c\|\hat{\boldsymbol{u}}\|_{1,\hat{E}}\|\hat{\boldsymbol{v}}\|_{\hat{E}}$$

for all $\hat{\boldsymbol{u}} \in H^1(\hat{E})^2$ and $\hat{\boldsymbol{v}} \in L_2(\hat{E})$. However, due to identity (3.26) we obtain, by a Bramble–Hilbert argument, the stronger bound

$$|\hat{a}_E(\hat{\Pi}\hat{\boldsymbol{u}}, (I - \hat{\Pi})\hat{\boldsymbol{v}})| \le c|\hat{\boldsymbol{u}}|_{1,\hat{E}} \|\hat{\boldsymbol{v}}\|_{\hat{E}}.$$

Hence, using (2.12) and the definition of a_h we obtain (4.6). ∎

Let $a(\boldsymbol{u}, \boldsymbol{v})$ be the continuous bilinear form $(\boldsymbol{K}^{-1}\boldsymbol{u}, \boldsymbol{v})$. The next result is a consistency result for the bilinear form a_h.

Lemma 4.3. *Let $\boldsymbol{u} \in (H^1)^2$ and $\boldsymbol{v} \in \mathcal{RT}_h^{1/2}$. Then there is a constant c, independent of h, such that*

$$|a_h(\Pi_h \boldsymbol{u}, \boldsymbol{v}) - a(\boldsymbol{u}, \boldsymbol{v})| \le ch\|\boldsymbol{u}\|_1 \|\boldsymbol{v}\|.$$

Proof. It follows from (3.28) that

$$|a(\boldsymbol{u}, \boldsymbol{v}) - (\boldsymbol{K}_h^{-1}\boldsymbol{u}, \boldsymbol{v})| = |(\boldsymbol{K}^{-1}\boldsymbol{u}, \boldsymbol{v}) - (\boldsymbol{K}_h^{-1}\boldsymbol{u}, \boldsymbol{v})| \le ch\|\boldsymbol{u}\|\|\boldsymbol{v}\|.$$

Hence, in order to complete the proof it is enough to show that

$$|a_h(\Pi_h \boldsymbol{u}, \boldsymbol{v}) - (\boldsymbol{K}_h^{-1}\boldsymbol{u}, \boldsymbol{v})| \le ch\|\boldsymbol{u}\|_1 \|\boldsymbol{v}\|. \tag{4.7}$$

However, by employing the identity (3.25) and the Bramble–Hilbert Lemma in an argument analog to the one in the proof of Lemma 4.2 above we obtain

$$|\hat{a}_E(\hat{\Pi}\hat{\boldsymbol{u}}, \hat{\boldsymbol{v}}) - (\mathcal{K}_E^{-1}\hat{\boldsymbol{u}}, \hat{\boldsymbol{v}})| \le c|\boldsymbol{u}|_{1,\hat{E}} \|\boldsymbol{v}\|_{\hat{E}}.$$

Therefore, (4.7) again follows from (2.12) and the definition of a_h. ∎

It is well known that, in addition to the boundedness of the bilinear forms, two corresponding Brezzi conditions have to be satisfied in order to ensure stability of a mixed finite element method of the form (3.29), cf. [11]. For the continuous mixed formulation (3.17) the proper function space for the formulation is $H(\mathrm{div}) \times L_2$. Hence, in the present setting the first Brezzi condition requires that

$$\sup_{\boldsymbol{v} \in \mathcal{RT}_h^{1/2}} \frac{(q, \mathrm{div}\, \boldsymbol{v})}{\|\boldsymbol{v}\|_{\mathrm{div}}} \ge \beta_1 \|q\| \qquad \text{for all } q \in Q_h, \tag{4.8}$$

where $\beta_1 > 0$ is independent of h. Since $\mathcal{RT}_h^{1/2} \supset \mathcal{RT}_h$, and the corresponding condition is well known to hold for the pair $\mathcal{RT}_h \times Q_h$, cf. [11, 23], we conclude that (4.8) is fulfilled.

The second stability condition is related to the weakly divergence free vector fields in $\mathcal{RT}_h^{1/2}$. Let Z_h denote the set of weakly divergence free vector fields, i.e.

$$Z_h = \{\boldsymbol{v} \in \mathcal{RT}_h^{1/2} : (\mathrm{div}\, \boldsymbol{v}, q) = 0, \quad \forall q \in Q_h\}.$$

The standard formulation of the second stability condition states that

$$\|\boldsymbol{v}\|_{\mathrm{div}} \le \beta_2 \|\boldsymbol{v}\| \qquad \text{for all } \boldsymbol{v} \in Z_h, \tag{4.9}$$

where β_2 is independent of h. This condition does not hold in present case since the elements of Z_h are not divergence free. However, if $\boldsymbol{v} \in Z_h \cap \mathcal{RT}_h$ then $\mathrm{div}\, v = 0$. This is seen by a transformation back to the reference space. Hence, for any $\boldsymbol{v} \in Z_h$ we must have that $\operatorname{div} \hat{\Pi}\hat{\boldsymbol{v}} = 0$. Therefore, the weaker condition

$$\|\boldsymbol{v}\| + \|\operatorname{div} \Pi_h \boldsymbol{v}\| \leq \beta_2 \|\boldsymbol{v}\| \qquad \text{for all } \boldsymbol{v} \in Z_h, \tag{4.10}$$

holds with constant $\beta_2 = 1$. This slight lack of stability for the mixed method (3.29) will have consequences for the error estimates we shall obtain. Instead of estimates in the norm of $H(\operatorname{div}) \times L_2$ we will instead obtain estimates in the weaker norm, were $\|\boldsymbol{v}\|_{\operatorname{div}}$ is replaced by $\|\boldsymbol{v}\| + \|\operatorname{div} \Pi_h \boldsymbol{v}\|$.

Remark. *The use of the norm* (4.10) *for the convergence analysis, seems to be consistent with numerical experiments, where one observes better behavior for the averaged edge flux compared to the half edge fluxes.*

A. The Error Estimates

Let $(\boldsymbol{u}, p) \in H(\operatorname{div}) \times L_2$ be the solution of the continuous problem (3.17) and $(\boldsymbol{u}_h, p_h) \in \mathcal{RT}_h^{1/2} \times Q_h$ the corresponding solution of (3.29). We assume that $\boldsymbol{u}$, $\operatorname{div} \boldsymbol{u}$, and p are all H^1 functions. Note that it follows from (3.20) that $\Pi_h(\boldsymbol{u} - \boldsymbol{u}_h) \in Z_h \cap \mathcal{RT}_h$ and therefore $\operatorname{div} \Pi_h(\boldsymbol{u} - \boldsymbol{u}_h) = 0$. We can therefore conclude from (4.3) that

$$\|\operatorname{div}(\boldsymbol{u} - \Pi_h \boldsymbol{u}_h)\| = \|\operatorname{div}(\boldsymbol{u} - \Pi_h \boldsymbol{u})\| \leq ch \|\operatorname{div} \boldsymbol{u}\|_1. \tag{4.11}$$

The L_2 part of $\boldsymbol{u} - \boldsymbol{u}_h$ is estimated next.

Lemma 4.4. *There is a constant c, independent of h, such that*

$$\|\boldsymbol{u} - \boldsymbol{u}_h\| \leq ch \|\boldsymbol{u}\|_1.$$

Proof. Due to the interpolation result (4.2) it is enough to show that

$$\|\Pi_h \boldsymbol{u} - \boldsymbol{u}_h\| \leq ch \|\boldsymbol{u}\|_1. \tag{4.12}$$

Furthermore, by (4.5) it is sufficient to estimate $a_h(\Pi_h \boldsymbol{u} - \boldsymbol{u}_h, \Pi_h \boldsymbol{u} - \boldsymbol{u}_h)^{1/2}$.

In order to do this we start by observing that since $\Pi_h(\boldsymbol{u} - \boldsymbol{u}_h)$ is divergence free it follows from the definition of $\boldsymbol{u}_h$ and (3.20) that

$$a_h(\boldsymbol{u}_h, \Pi_h \boldsymbol{u} - \boldsymbol{u}_h) = (p_h, \operatorname{div}(\Pi_h \boldsymbol{u} - \boldsymbol{u}_h)) = (p_h, \operatorname{div} \Pi_h(\boldsymbol{u} - \boldsymbol{u}_h)) = 0.$$

Hence,

$$\begin{aligned} a_h(\Pi_h \boldsymbol{u} - \boldsymbol{u}_h, \Pi_h \boldsymbol{u} - \boldsymbol{u}_h) &= a_h(\Pi_h \boldsymbol{u}, \Pi_h \boldsymbol{u} - \boldsymbol{u}_h) \\ &= a_h(\Pi_h \boldsymbol{u}, \Pi_h(\boldsymbol{u} - \boldsymbol{u}_h)) - a_h(\Pi_h \boldsymbol{u}, (I - \Pi_h)\boldsymbol{u}_h). \end{aligned}$$

Furthermore, since

$$a(\boldsymbol{u}, \Pi_h(\boldsymbol{u} - \boldsymbol{u}_h)) = (p, \operatorname{div}(\Pi_h(\boldsymbol{u} - \boldsymbol{u}_h))) = 0,$$

we have

$$a_h(\Pi_h \boldsymbol{u}, \Pi_h(\boldsymbol{u} - \boldsymbol{u}_h)) = a_h(\Pi_h \boldsymbol{u}, \Pi_h(\boldsymbol{u} - \boldsymbol{u}_h)) - a(\boldsymbol{u}, \Pi_h(\boldsymbol{u} - \boldsymbol{u}_h)).$$

We have therefore obtained the identity

$$a_h(\Pi_h \boldsymbol{u} - \boldsymbol{u}_h, \Pi_h \boldsymbol{u} - \boldsymbol{u}_h) = [a_h(\Pi_h \boldsymbol{u}, \Pi_h(\boldsymbol{u} - \boldsymbol{u}_h)) - a(\boldsymbol{u}, \Pi_h(\boldsymbol{u} - \boldsymbol{u}_h))] - a_h(\Pi_h \boldsymbol{u}, (I - \Pi_h)\boldsymbol{u}_h).$$

From the estimates of the Lemmas 4.2 and 4.3 we derive

$$
\begin{aligned}
a_h(\Pi_h \boldsymbol{u} - \boldsymbol{u}_h, \Pi_h \boldsymbol{u} - \boldsymbol{u}_h) &\leq ch\|\boldsymbol{u}\|_1 (\|\Pi_h(\boldsymbol{u} - \boldsymbol{u}_h)\| + \|(I - \Pi_h)\boldsymbol{u}_h\|) \\
&\leq ch\|\boldsymbol{u}\|_1 \|\Pi_h \boldsymbol{u} - \boldsymbol{u}_h\|,
\end{aligned}
$$

where the final inequality follows from (4.1). By (4.5) this implies (4.12). ∎

For the final estimate on $\|p - p_h\|$ it is, by (4.4), enough to bound $\|\mathcal{M}_h p - p_h\|$. The inf–sup condition on $\mathcal{RT}_h \times Q_h$ gives

$$
\begin{aligned}
\|\mathcal{M}_h p - p_h\| \leq & c \sup_{\boldsymbol{v} \in \mathcal{RT}_h} \frac{(\mathcal{M}_h p - p_h, \operatorname{div} \boldsymbol{v})}{\|\boldsymbol{v}\|_{\operatorname{div}}} \\
\leq & c \left\{ \|\mathcal{M}_h p - p\| + \sup_{\boldsymbol{v} \in \mathcal{RT}_h} \frac{(p - p_h, \operatorname{div} \boldsymbol{v})}{\|\boldsymbol{v}\|_{\operatorname{div}}} \right\} \\
\leq & c \left\{ \|\mathcal{M}_h p - p\| + \sup_{\boldsymbol{v} \in \mathcal{RT}_h} \frac{|a(\boldsymbol{u}, \boldsymbol{v}) - a_h(\Pi_h \boldsymbol{u}, \boldsymbol{v})| + a_h(\Pi_h \boldsymbol{u} - \boldsymbol{u}_h, \boldsymbol{v})}{\|\boldsymbol{v}\|_{\operatorname{div}}} \right\} \\
\leq & ch \left(\|p\|_1 + \|\boldsymbol{u}\|_1 \right)
\end{aligned}
$$

where we have used (4.4), (4.12) and Lemma 4.3.

Together with (4.11) and Lemma 4.4 this implies the following set of error estimates for the MPFA method.

Theorem 4.5. *Let $(\boldsymbol{u}, p)$ be the exact solution of (3.17) and $(\boldsymbol{u}_h, p_h) \subset \mathcal{RT}_h^{1/2} \times Q_h$ the solution of (3.29). There is a constant c, independent of h, but depending on $\|\boldsymbol{u}\|_1$, $\|\operatorname{div} \boldsymbol{u}\|_1$ and $\|p\|_1$, such that*

$$
\|\boldsymbol{u}_h - \boldsymbol{u}\| + \|\operatorname{div}(\Pi_h \boldsymbol{u}_h - \boldsymbol{u})\| + \|p_h - p\| \leq ch.
$$

V. CONCLUSIONS

This paper presents the MPFA method as a finite volume method which is equivalent to a mixed finite element method using a specific numerical quadrature. This provides a finite element setting in which the MPFA method can be understood and analyzed on quadrilateral grids. Optimal first order convergence is established for the Darcy velocity in a reduced $H(\operatorname{div})$ norm and for the pressure in the L_2–norm. The norm provides an estimate on the edge flux, as an average of the half edge fluxes. This seems to be consistent with numerical experiments, where one observes better behavior for the averaged edge flux compared to the half edge fluxes.

REFERENCES

1. I. Aavatsmark. An introduction to multipoint flux approximations for quadrilateral grids. *Comput. Geosci.*, 6:404–432, 2002.
2. I. Aavatsmark, T. Barkve, Ø. Bøe, and T. Mannseth. Discretization on non-orthogonal, curvilinear grids for multi-phase flow. *Proc. 4th European Conference on the Mathematics of Oil Recovery, Røros,*, D, 1994.

3. I. Aavatsmark, T. Barkve, Ø. Bøe, and T. Mannseth. Discretization on unstructured grids for inhomogeneous, anisotropic media. part i: Derivation of the methods. part ii: Discussion and numerical results. *SIAM J. Sci. Comput*, 19:1700–1736, 1998.

4. I. Aavatsmark, T. Barkve, and T. Mannseth. Control-volume discretization methods for 3D quadrilateral grids in inhomogeneous, anisotropic reservoirs. *SPE J.*, 3:146–154, 1998.

5. I. Aavatsmark, G. T. Eigestad, and R. A. Klausen. Numerical convergence of MPFA for general quadrilateral grids in two and three dimensions. *IMA Volumes in Mathematics and its Applications.*, 142, Compatible spatial discretizations for Partial Differential quations:1–22, 2006.

6. A. Agouzal, J. Baranger, J.-F. Maitre, and F. Oudin. Connection between finite volume and mixed finite element methods for a diffusion problem with nonconstants coefficients. application to a convection diffusion problem. *East-West J. Numer. Math.*, 3:237–254, 1995.

7. T. Arbogast, C. N. Dawson, P. T. Keenan, M. F. Wheeler, and I. Yotov. Enhanced cell-centered finite differences for elliptic equations on general geometry. *SIAM J. Sci. Comput*, 19:404–425, 1998.

8. D. N. Arnold, D. Boffi, and R. S. Falk. Quadrilateral H(div) finite elements. *SIAM J. Numer. Anal.*, 42:2429–2451, 2005.

9. M. Berndt, K. Lipnikov, J. D. Moulton, and M. Shashkov. Convergence of mimetic finite difference discretizations of the diffusion equation. *East-West J. Numer. Math.*, 9:130–148, 2001.

10. D. Braess. *Finite Elements*. Cambridge University Press, 1997.

11. F. Brezzi and M. Fortin. *Mixed and hybrid finite element methods*. Springer, New York, 1991.

12. S. Chou, D. Y. Kwak, and K. Y. Kim. A general framework for constructing and analyzing mixed finite volume methods on quadrilateral grids: The overlapping covolume case. *SIAM J. Numer. Anal.*, 39:1170–1196, 2001.

13. P. G. Ciarlet. *The Finite Element Method for Elliptic Problems*. Noth-Holland Publishing Company, 1997.

14. M. G. Edwards and C. F. Rogers. A flux continuous scheme for the full tensor pressure equation. *Proc. 4th European Conference on the Mathematics of Oil Recovery, Røros*, D, 1994.

15. M. G. Edwards and C. F. Rogers. Finite volume discretization with imposed flux continuity for the general tensor pressure equation. *Comput. Geosci.*, 2:259–290, 1998.

16. G. T. Eigestad, T. Aadland, I. Aavatsmark, R. A. Klausen, and J. M. Nordbotten. Recent advances for mpfa methods. *Proc. 9th European Conference on the Mathematics of Oil Recovery, Cannes, France*, 2004.

17. G. T. Eigestad and R. A. Klausen. On the convergence of the multi-point flux approximation o-method; numerical experiments for discontinous permeability. *Numer. Methods Partial Diff. Eqns*, 2(6):1079–10981, 2005.

18. R. E. Ewing, M. L. Liu, and J. Wang. Superconvergence of mixed finite element approximations over quadrilaterals. *SIAM J. Numer. Anal*, 36:772–787, 1999.

19. J. Hyman, M. Shashkov, and S. Steinberg. The numerical solution of diffusion problems in strongly heterogeneous non-isotropic materials. *J. Comput. Phys*, 132:254–316, 1997.

20. R. A. Klausen. *PhD thesis: On Locally Conservative Numerical Methods for Elliptic Problems; Application to Reservoir Simulation*. Dissertation, No 297. Unipub AS, Univ. of Oslo, 2003.

21. R. A. Klausen and T. F. Russell. Relationships among some locally conservative discretization methods which handle discontinuous coefficients. *Comput. Geosci*, 8:341–377, 2004.

22. Schlumberger. *Eclipse, Industry standard in reservoir simulation.* Schlumberger information solutions, 2003.

23. J. Wang and T. Mathew. Mixed finite element methods over quadrilaterals. *Proceedings of the 3th International Conference on Advances in Numerical Methods and Applications, Eds: I. T. Dimov, Bl. Sendov, and P. Vassilevskith.*, pages 203–214, 1994.

24. M. F. Wheeler and I. Yotov. A cell-centered finite difference method on quadrilaterals *IMA Volumes in Mathematics and its Applications.*, 142, Compatible spatial discretizations for Partial Differential quations:189–208, 2006.

25. M. F. Wheeler and I. Yotov. A multipoint flux mixed finite element method. Technical Report TR Math 05-06, Dept. Math., University of Pittsburgh, 2005. To appear.